CHAPTER V
MORPHOLOGY AND PHOTOPHYSICAL PROPERTIES OF ELECTROSPUN LIGHT-EMITTING POLYSTYRENE/ POLY(P-PHENYLENE ETHYNYLENE) FIBERS

5.1 Abstract

Ultra-thin fibers, consisting of blends of a PPE derivative and polystyrene, with average diameters ranging from 430 to 1,200 nm, were produced by electrospinning. The electrospinnability was significantly improved by adding pyridinium formate to the spinning solution. FT-IR spectroscopy was used to confirm the composition of the electrospun fibers and their morphology was probed by SEM. The optical properties of the as-prepared solutions, pristine and annealed fibers, and corresponding spin-coated and solution-cast films were investigated by UV-vis spectroscopy. A comparison of the PL emission spectra revealed aggregation of PPE molecules in the electrospun materials but the extent of aggregation can be reduced if the materials are annealed above the glass transition temperature.

(**Key-words**: Electrospinning; Photophysics; Polymer blend; Poly(*p*-phenylene ethynylene); Polystyrene)

5.2 Introduction

Since the discovery of the electrical conductivity in p-conjugated polymers thirty years ago,[1] (semi)conducting polymers have become the focus of intense research and development activities around the world.[2] Their use as synthetic metals[3] and as organic semiconductors in light-emitting diodes,[4] field-effect transistors,[5] photovoltaic devices,[6] sensors[7] and many other applications, has led to rapid growth of the field. Many different families of conjugated polymers, for example, poly(phenylene vinylene)s (PPVs),[8] poly(fluorene)s (PFs),[9] and poly(phenylene ethynylene)s (PPEs),[10] are being studied, often with the objective of tailoring their properties to meet the needs of these applications. PPE and its derivatives represent an interesting family because of their nonlinear optical characteristics,[11] photo-[12] and electroluminescent properties,[13] charge-carrier mobility,[14] and chemical responsiveness,[15] which make them attractive for use in applications that include organic light-emitting diodes,[16] light polarizers,[17] liquid crystal displays (LCDs),[18] transistors,[19] solar cells[20] and sensors.[21] Recently, cross-linked PPE networks[22] were demonstrated to be of a microporous nature with specific surface areas that exceed those of activated carbons and offer investigations with regards to the properties of PPEs have been in either solution or thin films, relatively little attention has been paid to the study of the polymers in the form of ultra-fine fibers, which offer high aspect and high surface area to volume or mass ratios.

Recently, Bunz and coworkers reported the investigation of the morphology and photophysical properties of electrospun (e-spun) poly(arylene ethynylene)s (PAEs) with dioctyl or polycaprolactone (PCL) side chains.[24] Interestingly, poly(2,5-dioctyl-p-phenylene ethynylene) with a degree of polymerization (DP) of 60 could only be sprayed into microspheres with average diameters of 1–1.5 μm, but not spun into fibers. On the other hand, grafting PCL chains with a DP of at least 65 to either a poly(p-phenylene ethynylene) or poly(benzothiadiazoleco-alkyne-co-benzene-co-alkyne) core resulted in materials that could, under optimized conditions, be spun into welldefined fibers with diameters ranging from 50 nm to 1 μm. The

nature of the solvent, the concentration of the polymer in the spinning solution, and the DPs of the PCL side chains and the PAE core were all found to play a major role in determining the morphology of the electrospun products obtained. Most importantly, the high-molecular-weight PCL side chains employed by Bunz contribute significantly to the viscosity of the solution, allowing electrospinning (e-spinning) of high-quality fibers.[24] On the other hand, e-spinning of a more common PPE derivative (i.e., one in which the electrospinnability is not imparted through high molecular weight side chains) into fiber form has not yet been reported. This appears directly related to rheological limitations.[25–32] PAEs are often produced as materials of rather low-molecular weight, sometimes deliberately to maintain good solubility,[12a] so that even at their solubility limit they form solutions of low viscosity.[24]

We here report an approach that is orthogonal to the high-DP side chain route, namely the e-spinning of blends of a common poly(2,5-dialkoxy-p-phenylene ethynylene) derivative featuring an alternate substitution of ethylhexyloxy and octyloxy in the 2 and 5 positions of the phenylene rings (EHO-OPPE;[12a] see Figure 5.1) and polystyrene (PS) as an 'inert' carrier polymer. We demonstrate that this approach allows one to produce ultra-fine fibers with diameters that range from hundreds of nanometers to one micrometer.

5.3 Experimental

5.3.1 Materials and Preparation of Solutions for Spinning and Casting Films

EHO-OPPE ($M_n \approx 14{,}000$ Da; Figure 5.1) was synthesized following a procedure previously described.[12a] PS ($M_w \approx 3.0 \times 10^5$ Da; pellet form) was a general purpose grade from Dow Chemicals (USA). The solvents used were 1,2-dichloroethane [DCE; Lab-Scan (Asia), Thailand] and chloroform (CF; Carlo Erba, Italy). Pyridinium formate (PF), a volatile organic salt, was prepared by reacting pyridine [Lab-Scan (Asia), Thailand] and formic acid (Merck, England) in an equimolar quantity. Solutions of 8.5% (w/v) PS/EHO-OPPE in DCE or CF (the

compositional weight ratio between PS and EHO-OPPE being 7.5:1) with or without the addition of 8 vol.-% PF were prepared by combining all compounds and stirring at room temperature for 5 min. A solution of 8.5% (w/v) PS in DCE was prepared in similar fashion and was used as a reference.

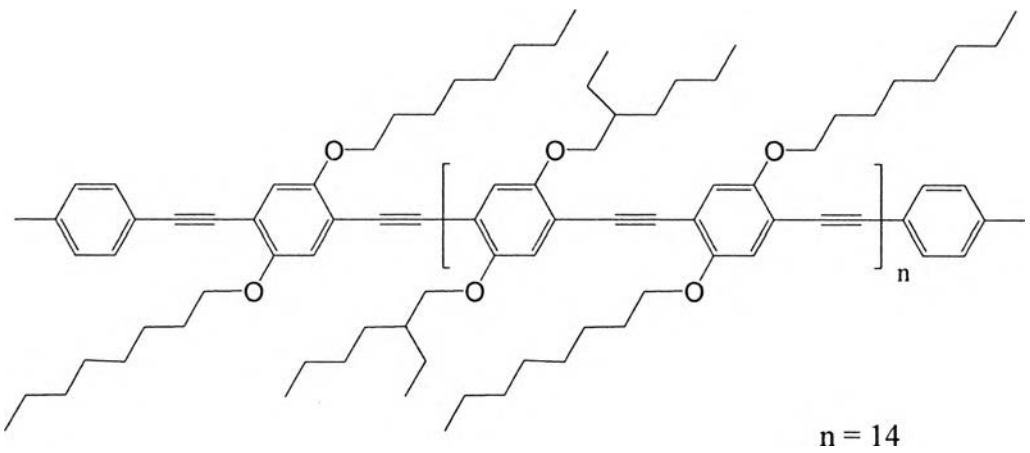

Figure 5.1 Chemical structure of EHO-OPPE, the PPE derivative used.

5.3.2 Electrospining

E-spinning of the as-prepared solutions was carried out under an electrical potential of between 7.5 and 20 kV. Unless otherwise indicated, products (i.e., fibers and/or beads) were spun at an applied electrical potential of 15 kV. The collection distance and the collection time were fixed at 10 cm and 1 min, respectively. Each of the freshly-prepared spinning solutions was placed in a 5 mL plastic syringe, the open end of which was connected to a blunt 20 gauge stainless steel hypodermic needle (outer diameter = 0.91 mm), which was used as the nozzle. An aluminum foil wrapped around a rigid plastic sheet was used as the collector plate. The emitting electrode of positive polarity from a Gamma High-Voltage Research ES30P DC power supply (Florida, USA) was connected to the needle, while the grounding electrode was connected to the collector plate. The feed rate of the solution was controlled by means of a Kd Scientific syringe pump at 1 $mL \cdot h^{-1}$. Where applicable, the e-spun fibers were annealed for between 5 min and 1 h at 110 °C, which is above the glass transition temperature (Tg) of PS (95 °C[33]).

5.3.3 Spin-Coating and Solution-Casting

Films of the PS/EHO-OPPE blends were produced by either spin coating or solution casting from solutions comprising 8–10 $mg \cdot mL^{-1}$ of the polymer blend. Spin coating was done on a Specialty Coating Systems model P6700 with spinning speeds of 1,500–2,000 rpm to achieve a final thickness of 0.5–1 μm. Solution casting was done on glass slides and resulted films of a final thickness of 1–3 μm.

5.3.4 Characterizations

The morphological appearance of the e-spun fibers was examined by a JEOL JSM-5410LV scanning electron microscope (SEM). The average bead diameters and the number of beads per unit area (i.e., the bead density) of the electrosprayed beads or the e-spun beaded fibers were calculated from measurements of SEM images at ×500 magnification. Diameters of the e-spun fibers, where applicable, were determined from SEM images at ×1,000 magnification, with the average value being calculated from at least 50 measurements (for each spinning condition). For beaded fibers, only the diameters of the fiber segments between beads were measured. A Thermo-Nicolet Nexus 670 Fourier-transform infrared (FT-IR) spectroscope was used to characterize the as-received PS pellets, the as-synthesized EHO-OPPE, and some of the e-spun PS/EHO-OPPE products. Optical absorption and photoluminescence emission spectra of the PS/EHO-OPPE solutions in DCE and CF with or without PF addition, the corresponding pristine and annealed e-spun fibers, spin-coated films, and solution-cast films were measured by a Hewlett Packard-8254A diode array UV-vis spectrophotometer (UV-vis) and a Perkin-Elmer LS50 luminescence spectrometer (PL). For the solution measurements, a 1 mm thick quartz cuvette was used in order to reduce the self-absorption effect, allowing the detection of photon emission from front surface. For PL experiments, samples were excited at 400 nm.

5.4 Results and discussion

5.4.1 Morphology of the E-spun Products Spun from PS, PS/EHO-OPPE, and PS/EHO-OPPE Added PF Solutions

Polystyrene (PS), a non-luminescent glassy-amorphous polymer, was chosen as an 'inert' carrier polymer for the present study. Neat PS was e-spun for reference purposes from 1,2-dichloroethane (DCE) to determine the morphology of the neat polymer template when processed under the conditions selected for this study. Figure 5.2 shows representative SEM images of the products obtained from a 8.5% (w/v) solution of PS in DCE under various electrical potentials between 7.5 and 20 kV. The e-spinning of a 8.5% (w/v) PS solution in DCE only resulted in the formation of beads, with average size in the range of 22.6–29.0 μm (see Figure 5.2 and Table 5.1). The density of the beads on the collection plate was between 0.17×10^5 and 0.56×10^5 beads·cm^{-2}. This tendency to form beads rather than ultra-fine fibers was previously observed and reported for PS that was e-spun from DCE or chloroform (CF), the second solvent employed here, if the concentration of the PS solutions was less than 10 wt.-%.[34]

Interestingly, the electro-spinnability of the PS solution in DCE was significantly improved in the presence of a comparably small amount of FHO-OPPE [i.e., PS:EHO-OPPE = 7.5:1 (w/w)]. Representative SEM images of the e-spun products (see Figure 5.3a) clearly show the appearance of ultra-fine fibers with a limited density of elongated beads. The average fiber diameters, bead size, and bead density of the beaded fibers obtained are in the range of 0.43–0.83 μm, 2.77–3.65 μm and 1.43×10^5–3.77×10^5 beads·cm^{-2}, respectively (see Table 5.1). To further improve the electro-spinnability of the PS/EHO-OPPE solution, the volatile organic salt pyridinium formate (PF) was added.[32] Figure 5.3b shows representative SEM images of the e-spun products. Either smooth or beaded fibers with fewer beads were observed. The average fiber diameter range increased to 0.55–0.87 μm, while the bead size range remained about the same at 2.12–4.89 μm. However, the bead density range decreased to 0.04×10^5–1.32×10^5 beads·cm^{-2}. This substantial

decrease in the bead density shows that the addition of PF helps to promote uniform fiber formation.

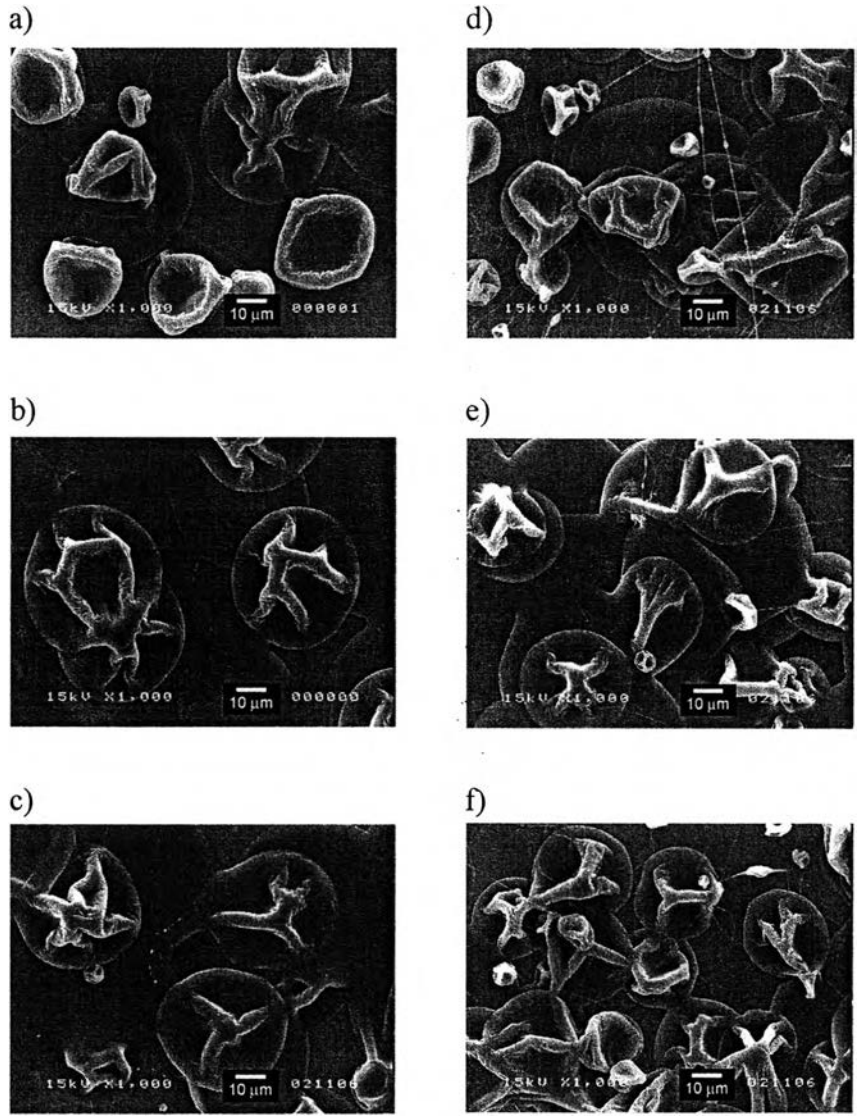

Figure 5.2 SEM images of the electrosprayed PS beads from 8.5% (w/v) solutions of PS in DCE (×1000, scale bar = 10 μm). The applied electrical potential for the electrospinning was: a) 7.5, b) 10, c) 12.5, d) 15, e) 17.5, and f) 20 kV.

Table 5.1 Average fiber diameter, bead size and bead density of the electrospun products from 8.5% (w/v) solutions of PS in DCE and 8.5% (w/v) solutions of PS/EHO-OPPE (PS:EHO-OPPE = 7.5:1) in DCE and CF without and with the addition of 8 vol.-% PF. The table lists parameters for materials e-spun at different applied electrical potentials (HV). The collection distance was 10 cm, the collection time was 1 min and the solution flow rate was 1 $mL \cdot h^{-1}$

Solution	HV (kV)	Fiber Diameters (μm)	Bead Size (μm)	Bead Density (beads·cm^{-2})
PS/DCE	7.5	-	29.05 ± 11.53	0.34×10^5
	10.0	-	28.12 ± 12.24	0.17×10^5
	12.5	-	27.94 ± 13.94	0.36×10^5
	15.0	-	22.57 ± 14.86	0.56×10^5
	17.5	-	26.92 ± 11.81	0.29×10^5
	20.0	-	24.37 ± 12.08	0.45×10^5
PS/EHO-OPPE /DCE	7.5	0.43 ± 0.14	2.88 ± 0.71	3.77×10^5
	10.0	0.54 ± 0.21	2.77 ± 0.75	3.52×10^5
	12.5	0.61 ± 0.17	3.65 ± 1.02	2.86×10^5
	15.0	0.79 ± 0.21	3.18 ± 1.08	2.00×10^5
	17.5	0.81 ± 0.18	3.11 ± 1.22	1.59×10^5
	20.0	0.83 ± 0.18	2.91 ± 0.85	1.43×10^5
PS/EHO-OPPE /DCE + PF	7.5	0.55 ± 0.12	2.12 ± 0.51	0.04×10^5
	10.0	0.66 ± 0.19	2.96 ± 0.93	0.57×10^5
	12.5	0.70 ± 0.15	3.58 ± 0.96	0.40×10^5
	15.0	0.72 ± 0.24	4.89 ± 1.56	1.32×10^5
	17.5	0.76 ± 0.28	4.74 ± 2.85	1.25×10^5
	20.0	0.87 ± 0.28	4.82 ± 2.08	1.20×10^5

Table 5.1 (Cont.) Average fiber diameter, bead size and bead density of the electrospun products from 8.5% (w/v) solutions of PS in DCE and 8.5% (w/v) solutions of PS/EHO-OPPE (PS:EHO-OPPE = 7.5:1) in DCE and CF without and with the addition of 8 vol.-% PF. The table lists parameters for materials e-spun at different applied electrical potentials (HV). The collection distance was 10 cm, the collection time was 1 min and the solution flow rate was 1 $mL \cdot h^{-1}$

Solution	HV (kV)	Fiber Diameters (μm)	Bead Size (μm)	Bead Density (beads·cm^{-2})
PS/EHO-OPPE /CF	7.5	0.51 ± 0.12	13.65 ± 0.65	4.13×10^5
	10.0	0.56 ± 0.12	14.05 ± 0.80	4.23×10^5
	12.5	0.63 ± 0.14	15.14 ± 0.82	5.25×10^5
	15.0	0.66 ± 0.15	16.11 ± 1.19	2.76×10^5
	17.5	0.68 ± 0.20	17.80 ± 1.31	2.82×10^5
	20.0	0.68 ± 0.15	18.05 ± 1.23	2.46×10^5
PS/EHO-OPPE /CF + PF	7.5	1.04 ± 0.33	1.06 ± 0.55	0.66×10^5
	10.0	1.04 ± 0.39	4.24 ± 1.84	2.26×10^5
	12.5	1.05 ± 0.37	4.41 ± 2.21	1.71×10^5
	15.0	1.12 ± 0.53	5.00 ± 2.64	1.51×10^5
	17.5	1.16 ± 0.38	5.23 ± 2.24	1.47×10^5
	20.0	1.20 ± 0.37	5.76 ± 3.74	1.36×10^5

The same trends were observed when CF was used as the solvent (see Figure 5.4a and b). In this case, the average fiber diameters, bead sizes, and bead densities of the e-spun PS/EHO-OPPE fibers from the blend solution without the addition of PF are in the range of 0.51–0.68 μm, 13.65–18.05 μm and 2.46×10^5–5.25×10^5 beads·cm^{-2}, respectively (see Table 5.1). Here, the addition of PF in the blend solution also resulted in an observed increase of the average fiber diameters in the range of 1.04–1.20 μm and an observed decrease of the bead density in the range of 0.66 × 105–1.71×10^5 beads·cm^{-2}. On the other hand, the bead size was found to decrease in the range of 1.06–5.76 μm (see Table 5.1).

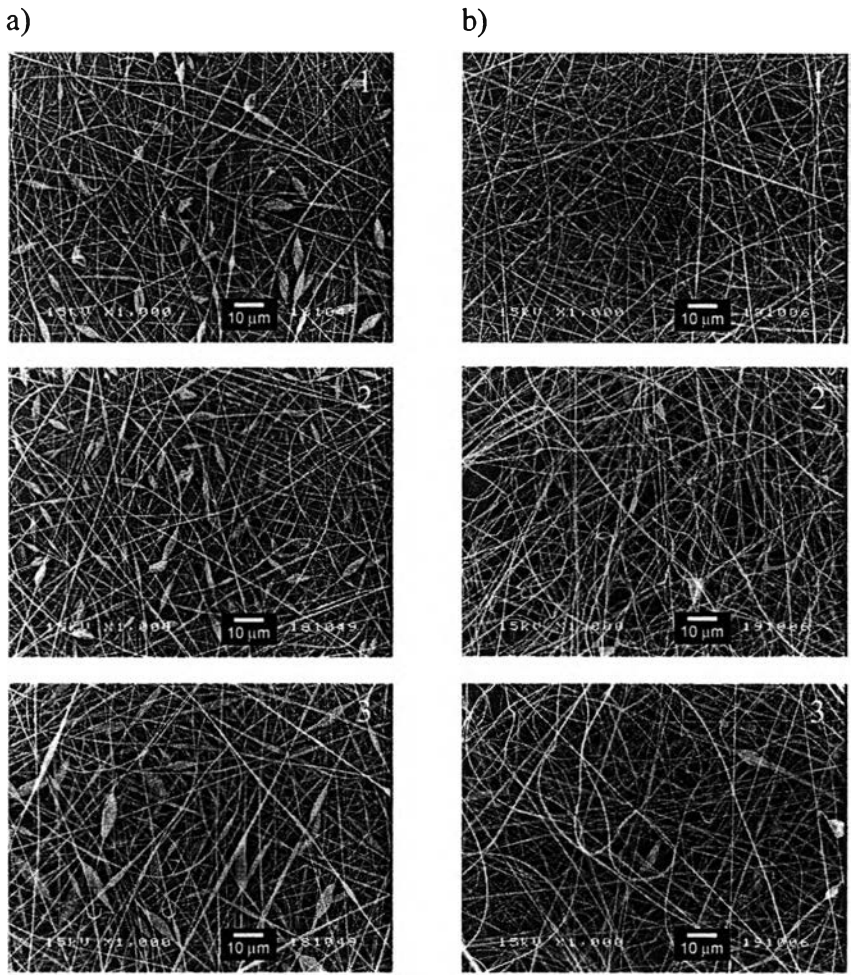

Figure 5.3 SEM images of the electrospun products from 8.5% (w/v) solutions of PS/EHO-OPPE (PS:EHO-OPPE = 7.5:1) in DCE without (a) and with (b) the addition of 8 vol.-% PF (×1,000, scale bar = 10 μm). The applied electrical potential for the electrospinning was (1) 7.5, (2) 10, (3) 12.5, (4) 15, (5) 17.5 and (6) 20 kV.

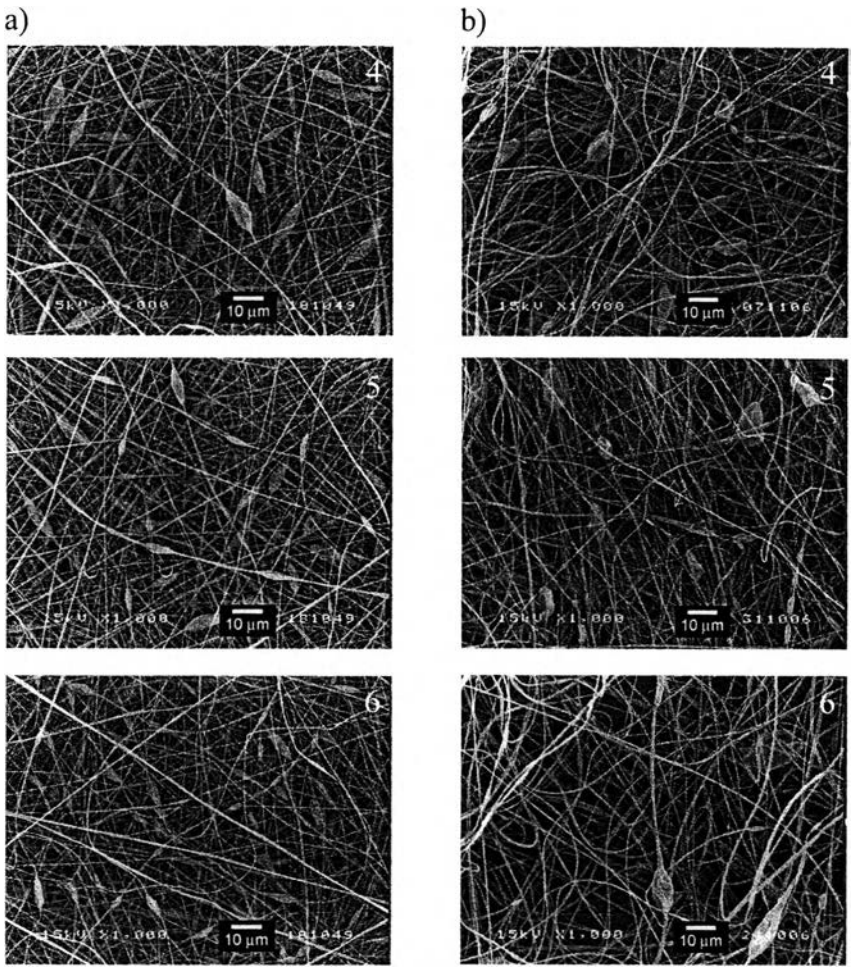

Figure 5.3 (cont.) SEM images of the electrospun products from 8.5% (w/v) solutions of PS/EHO-OPPE (PS:EHO-OPPE = 7.5:1) in DCE without (a) and with (b) the addition of 8 vol.-% PF (×1,000, scale bar = 10 µm). The applied electrical potential for the electrospinning was (1) 7.5, (2) 10, (3) 12.5, (4) 15, (5) 17.5 and (6) 20 kV.

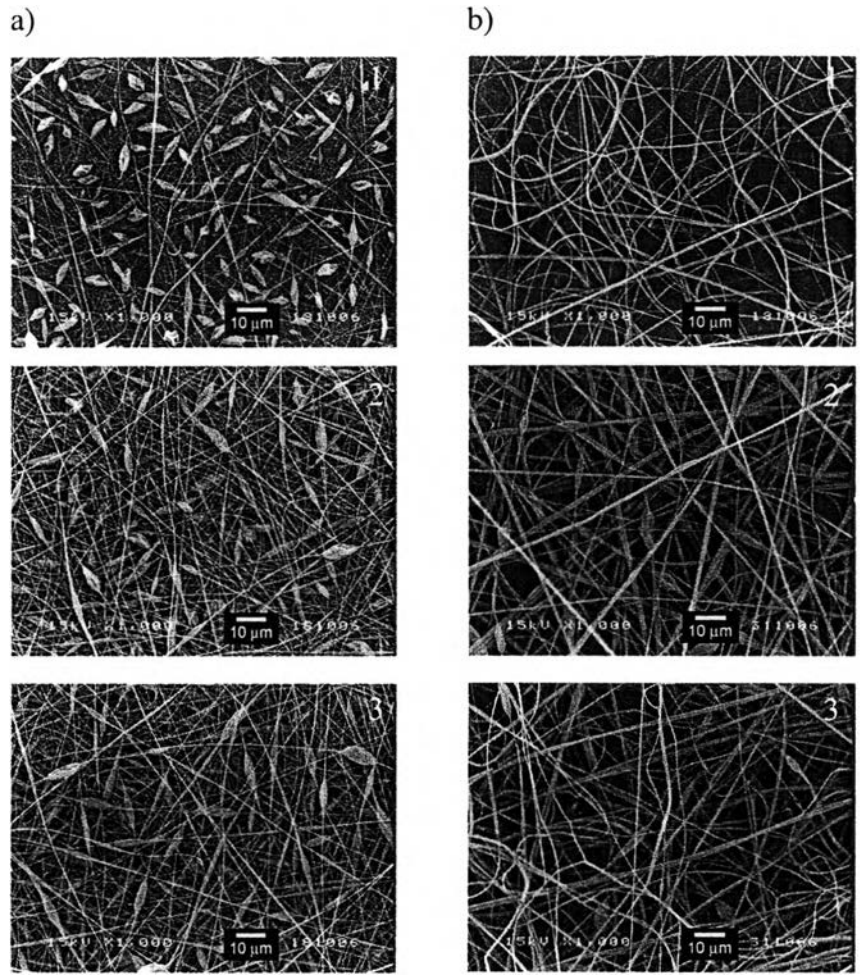

Figure 5.4 SEM images of the electrospun products from 8.5% (w/v) solutions of PS/EHO-OPPE (PS:EHO-OPPE = 7.5:1) in CF without (a) and with (b) the addition of 8 vol.-% PF (×1,000, scale bar = 10 μm). The applied electrical potential for the electrospinning was (1) 7.5, (2) 10, (3) 12.5, (4) 15, (5) 17.5 and (6) 20 kV.

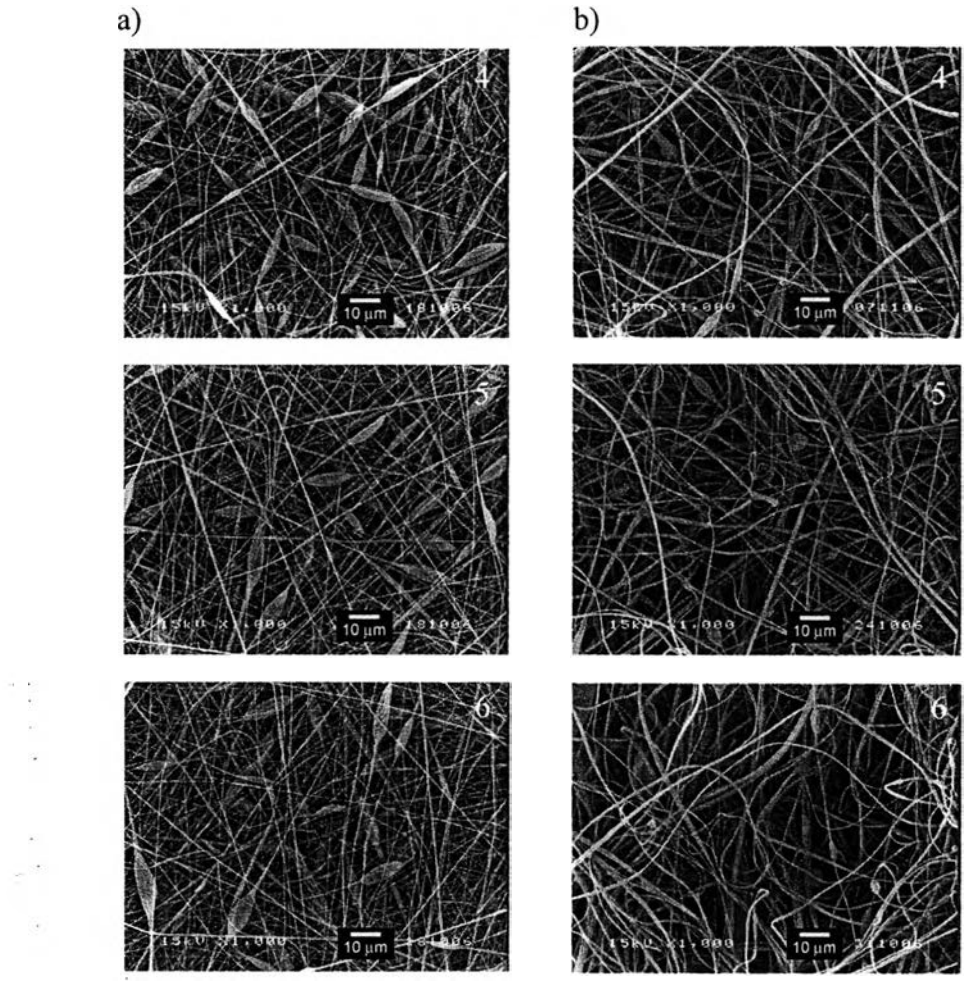

Figure 5.4 (cont.) SEM images of the electrospun products from 8.5% (w/v) solutions of PS/EHO-OPPE (PS:EHO-OPPE = 7.5:1) in CF without (a) and with (b) the addition of 8 vol.-% PF (×1,000, scale bar = 10 μm). The applied electrical potential for the electrospinning was (1) 7.5, (2) 10, (3) 12.5, (4) 15, (5) 17.5 and (6) 20 kV.

Based on these results, it appears that DCE is a better solvent than CF for the e-spinning of the blend solution of PS and EHO-OPPE, because the average fiber diameters, bead sizes, and bead densities of the products obtained from the blend solutions – with and without PF – in DCE are lower than those of the products obtained from the corresponding blend solutions in CF. Based on the quantitative results summarized in Table 5.1, it is evident that the average diameter of the e-spun fibers increases with increasing applied electrical potential. This is a direct result of

the increase in the total number of charged species within the jet segment, which, in turn, causes an increase in the electrostatic forces. The increase in such forces leads to an increase in the speed of the jet and a hypothetic decrease in the total path trajectory of the jet, which results in an increase in the feed flow rate and ultimately the diameters of the obtained fibers.[35,36] Clearly, the addition of PF to the spinning solution also improves significantly the electro-spinnability of the spinning solution, as shown from the substantial decrease in the bead density (see Table 5.1). In view of previous studies, which based the results on an increase in the number of charge carriers within the jet due to the addition of PF, this result does not come as a surprise.[35,37,38]

5.4.2 Chemical Integrity of E-spun Products Spun from PS, PS/EHO-OPPE, and PS/EHO-OPPE Added PF Solutions

FT-IR spectroscopy was conducted to confirm the existence of both PS and EHO-OPPE constituents in the e-spun blend fibers (see Figure 5.5). Individual spectra are shown of the as-received PS, the as-synthesized EHO-OPPE, and the selected fiber mats which had been e-spun from 8.5% (w/v) solution of PS in DCE and 8.5% (w/v) solutions of PS/EHO-OPPE in DCE or CF with and without the addition of PF at an electrical potential of 15 kV. Table 5.2 summarizes some absorption peaks specific to chemical functionalities of the PS and the EHO-OPPE components in the e-spun fibers. Clearly, the peaks characteristic to the PS component are observed in all of the FT-IR spectra of the e-spun fibers (i.e., at 697–698, 754–756, 906, 1 490, 2,920, 3,030 and 3,060 cm^{-1}). Moreover, some peaks characteristic to the EHO-OPPE component (e.g., at 1,210 and 1,270 cm^{-1}) are also observed in the FT-IR spectra of the e-spun fibers. The peak at 1,210 cm^{-1} corresponds to ring stretching vibrations and C–H deformation, while the peak at 1,270 cm^{-1} is specific to aryl alkyl ether (C–O–C) asymmetric stretching vibrations. These results confirm the existence and the chemical integrity of both the PS and the EHO-OPPE components in the e-spun fibers.

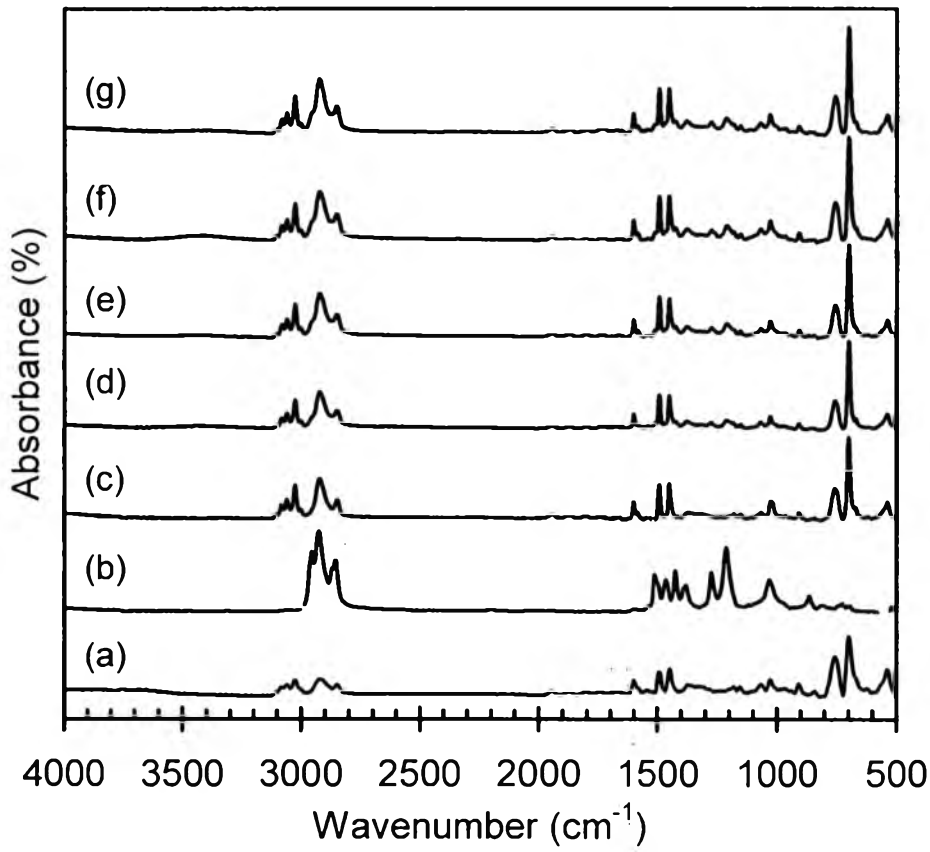

Figure 5.5 FT-IR spectra of a) as-received neat PS, b) EHO-OPPE powder, and the electrospun fibers from, c) 8.5% (w/v) solution of PS in DCE, 8.5% (w/v) solutions of PS/EHO-OPPE (PS:EHO-OPPE = 7.5:1) in DCE without d) and with e) the addition of 8 vol.-% PF, and 8.5% (w/v) solutions of PS/EHO-OPPE (PS:EHO-OPPE = 7.5:1) in CF without f) and with g) the addition of 8 vol.-% PF.

Table 5.2 Analysis of FT-IR spectra of as-received PS, EHO-OPPE and the electrospun products from 8.5% (w/v) solutions of PS in DCE and 8.5% (w/v) solutions of PS/EHO-OPPE (PS:EHO-OPPE = 7.5:1) in DCE and CF without and with the addition of 8 vol.-% PF

Absorption Band (cm^{-1})							Assignment
As-received Materials		Electrospun Products					
PS	EHO-OPPE	PS/ DCE	PS/ EHO-OPPE/ DCE	PS/ EHO-OPPE/ DCE + PF	PS/ EHO-OPPE/ CF	PS/ EHO-OPPE/ CF + PF	
698	-	698	697	697	697	697	CH bending vibrations in CH deformation
754	-	756	755	756	755	756	CH out-of-plane bending vibrations in -CH=CH-(cis) group
-	863	-	-	-	-	-	CH out-of-plane bending vibrations in $C=CH_2$ group
906	-	906	906	906	905	905	CH out-of-plane bending vibrations in $-CH=CH_2$ group
-	1,030	1,030	1,030	1,030	1,030	1,030	Aryl alkyl ether (C-O-C) symmetric stretching vibrations
-	1,210	-	1,210	1,210	1,210	1,210	Ring-stretching vibrations and CH deformation
-	1,270	-	1,270	1,270	1,270	1,270	Aryl alkyl ether (C-O-C) asymmetric stretching vibrations
-	1,380	-	-	-	-	-	CH bending vibrations in $-CH_3$ deformation
-	1420	-	-	-	-	-	CH bending vibrations in $-CH_2$ and $-CH_3$ deformation
1,450	1,470	1,450	1,450	1,450	1,450	1,450	Asymmetric CH bending vibrations in $-CH_3$ group
1,490	-	1,490	1,490	1,490	1,490	1,490	CH bending vibrations in $-CH_2$ Scissoring group
1,600	1,510	1,600	1,600	1,600	1,600	1,600	C=C stretching vibrations in Conjugated
2,850	2,860	2,850	2,850	2,850	2,850	2,850	Symmetric CH stretching vibrations in $-CH_2$ group
2,920	-	2,920	2,920	2,920	2,920	2,920	Asymmetric CH stretching vibrations in $-CH_2$ group
-	2,930	-	-	-	-	-	Asymmetric CH stretching vibrations in $-CH_3$ group
-	2,960	-	-	-	-	-	Asymmetric CH stretching vibrations in $-CH_3$ group
3,030	-	3,020	3,020	3,020	3,020	3,020	CH stretching vibrations in =C-H, $=CH_2$ and CH groups
3,060	-	3,060	3,060	3,060	3,060	3,060	CH stretching vibrations in =C-H, $=CH_2$ and CH groups

5.4.3 Optical Properties of the Spinning Solutions, Pristine and Annealed E-spun Fibers, and Spin-coated and Solution-cast Reference Films

The optical properties of the spinning solutions, pristine and annealed e-spun fibers, and spin-coated and solution-cast reference films were investigated by UV-Vis absorption and PL spectroscopy and the results are summarized in Table 5.3. Figure 5.6a and b summarize the optical properties of the 8.5% (w/v) spinning solutions of PS/EHO-OPPE (7.5:1 w/w) in DCE and CF with and without 8 vol.-% PF. All spectra were normalized to allow for easy comparison. The emission spectra of 8.5% (w/v) solutions of PS/EHO-OPPE in DCE exhibit sharp peaks at 487 and 508 nm (see Figure 5.6b). The emission spectra of 8.5% (w/v) solutions of PS/EHO-OPPE in CF are almost identical, displaying maxima at 485 and 507 nm, respectively (see Figure 5.6b). While the solvent has a slight solvatochromic effect on the absorption and the emission maxima of EHO-OPPE in DCE and CF, the addition of PS and PF does not exert any appreciable influence on the optical characteristics of the conjugated polymer. The features – splitting of the emission spectra into two well-resolved bands and the lack of mirror image similarity between absorption and emission – are related to vibronic coupling and are characteristic of alkyloxy-PPE emission.[12a]

Figure 5.7a and b show the emission spectra of fibers spun from 8.5% (w/v) solutions of PS/EHO-OPPE with 8 vol.-% PF in DCE and CF, respectively, as a function of the applied electrical potential. All emission spectra exhibit a broad peak centered around 508–519 nm and weak shoulders around 457–461 and 590–599 nm. Compared to the emission spectra of the spinning solutions, the emission spectra of the e-spun fibers show less-well-resolved features and appear somewhat broadened, indicative of aggregation of the conjugated polymer guest in the PS matrix. While the PL spectra of the fibers that had been e-spun at different electrical potential exhibit minor differences (see Table 5.4), there is no specific correlation between the emission peak positions and the applied electrical potential. It is postulated that the slight variation in the emission peak positions occurs from the fluctuation in the forces acting on jet segments, and hence the EHO-OPPE molecules, during the e-spinning.

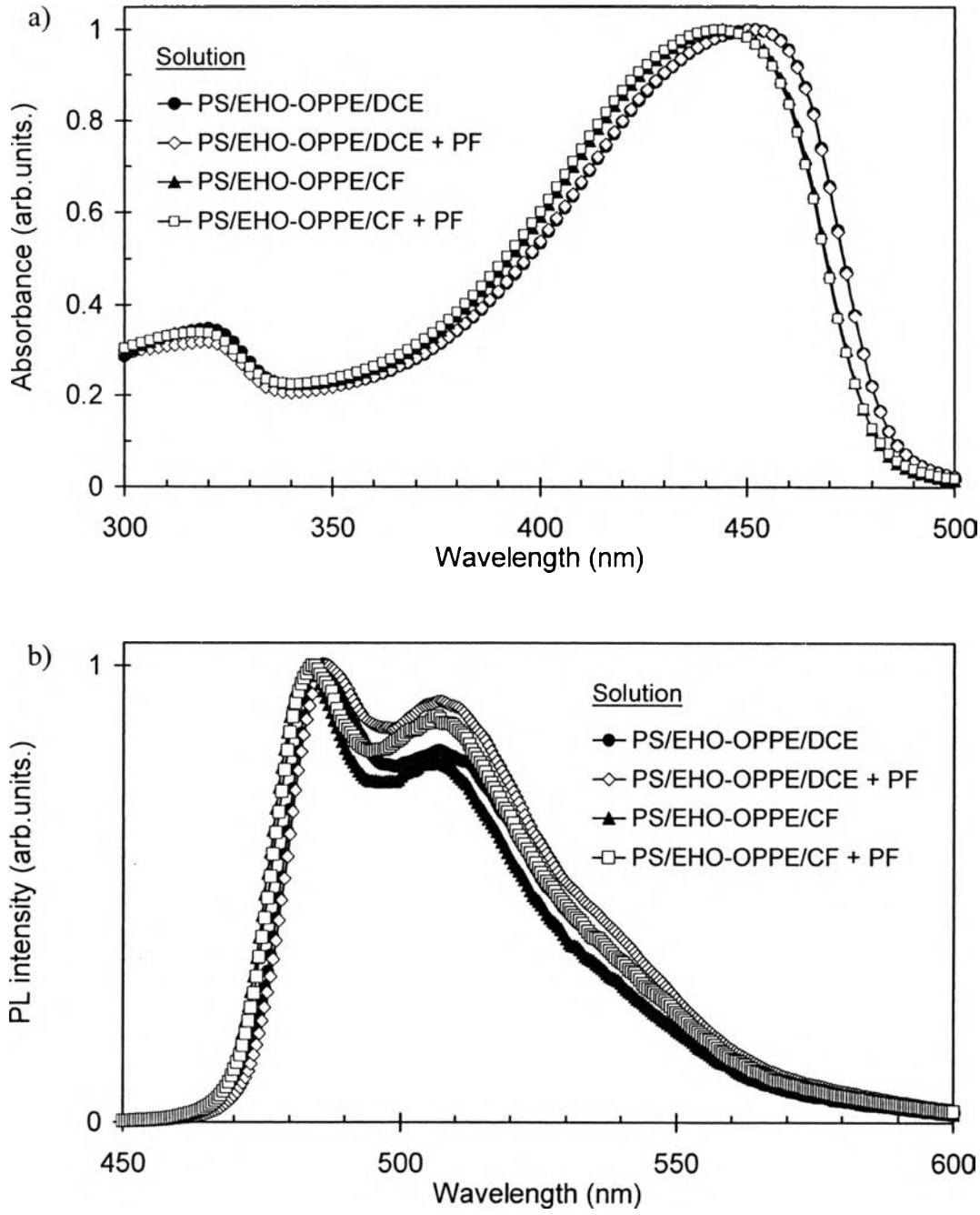

Figure 5.6 a) Absorption and b) PL emission spectra of 8.5% (w/v) solutions of PS/EHO-OPPE (PS:EHO-OPPE = 7.5:1) in DCE and 8.5% (w/v) solutions of PS/EHO-OPPE (PS:EHO-OPPE = 7.5:1) in CF without and with the addition of 8 vol.-% PF.

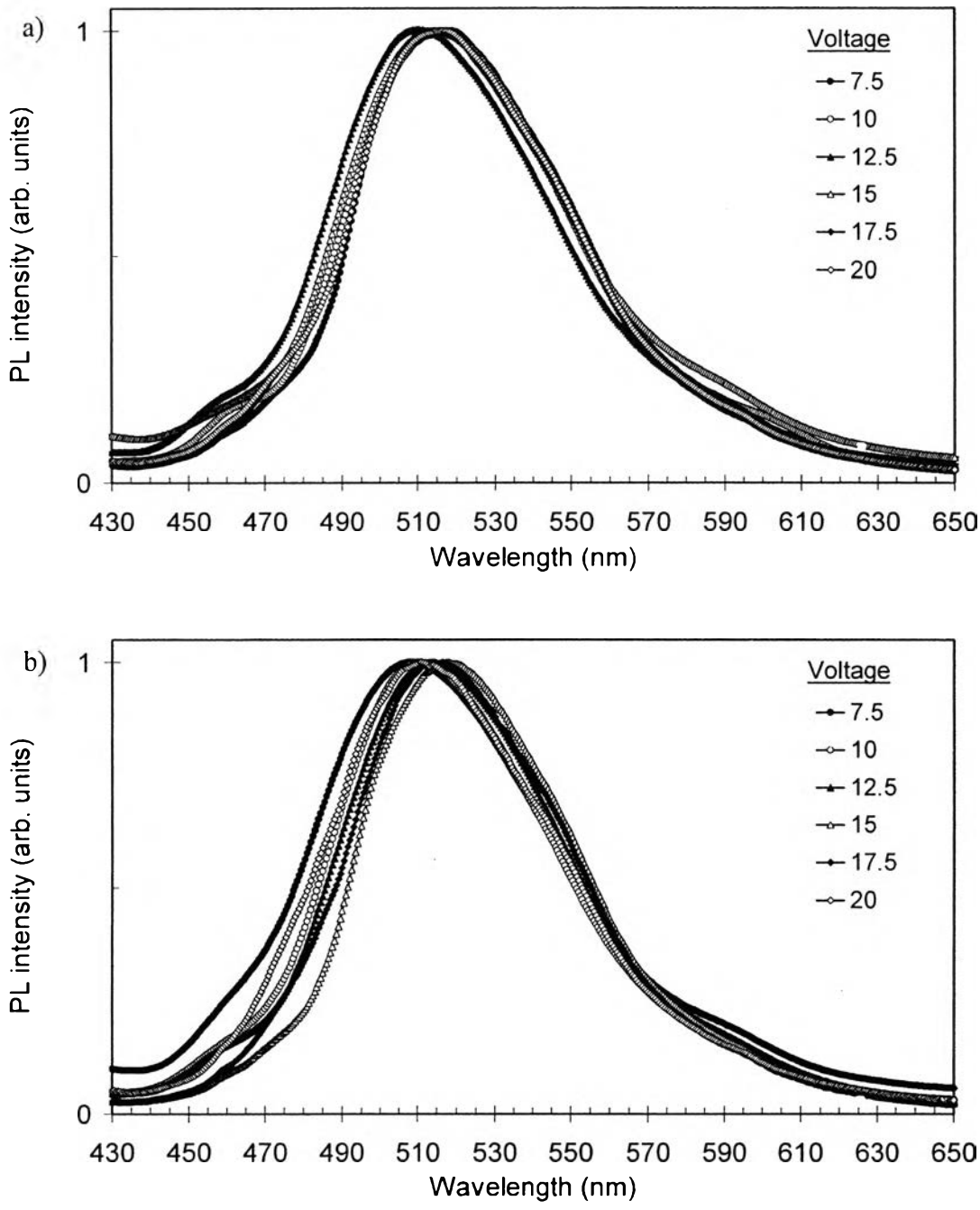

Figure 5.7 PL emission spectra of the electrospun fibers from 8.5% (w/v) solutions of PS/EHO-OPPE (PS:EHO-OPPE = 7.5:1) with the addition of 8 vol.-% PF in a) DCE, and b) CF at various applied electrical potentials.

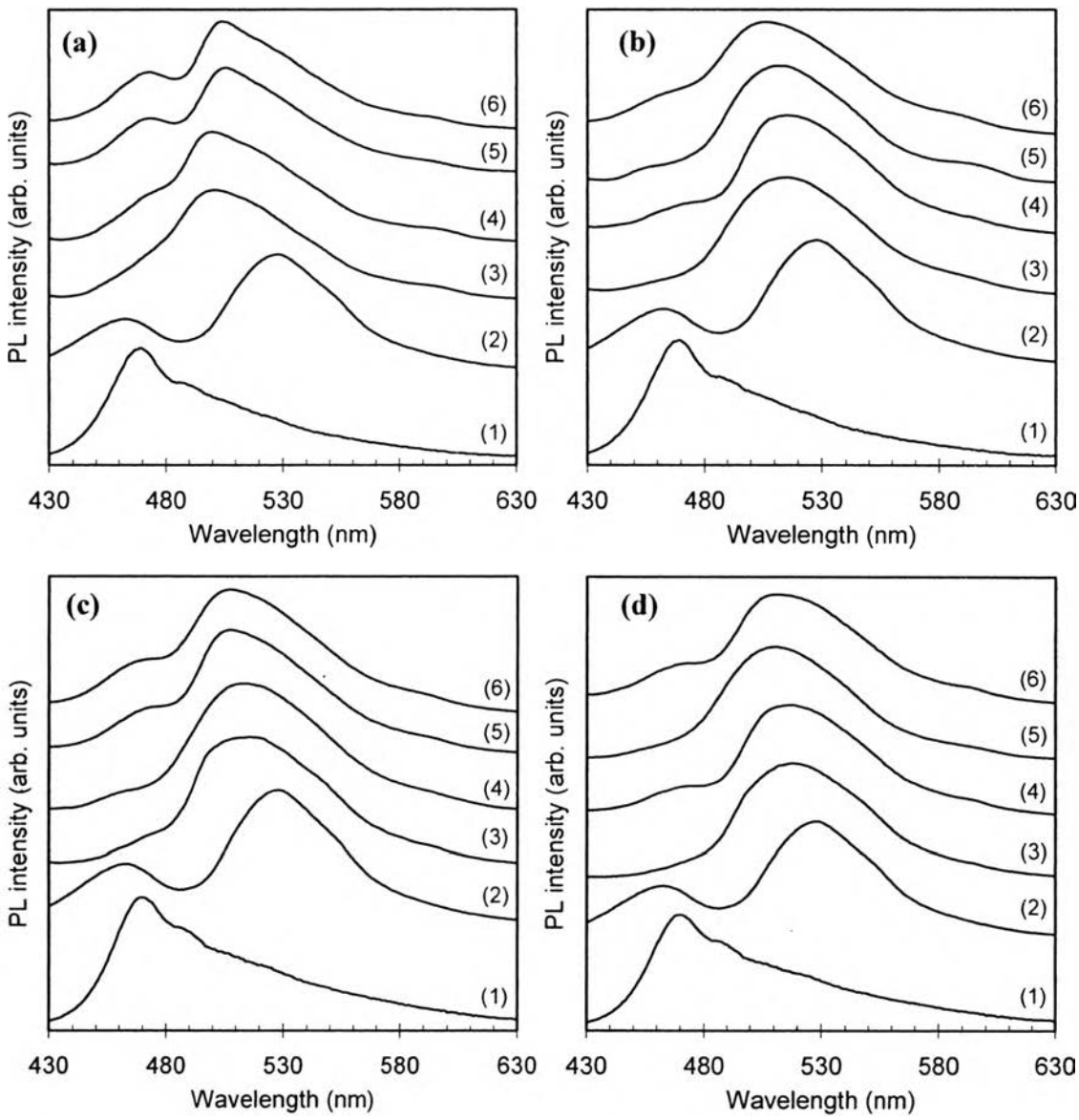

Figure 5.8 Emission spectra of samples produced from solutions of 8.5% (w/v) PS/EHO-OPPE (PS:EHO-OPPE = 7.5:1) in a) DCE, b) DCE with the addition of 8 vol.-% PF, c) CF and d) CF with the addition of 8 vol.-% PF. Samples were (1) spin-coated films, (2) solution-cast films, (3) pristine e-spun fibers, and e-spun fibers annealed at 110 °C for (4) 5 min, (5) 30 min, and (6) 1 h.

For the purpose of comparison, the emission characteristics of films prepared by spin-coating and solution-casting of 8.5% (w/v) solutions of PS/EHO-OPPE in DCE and CF with and without 8 vol.-% PF were also investigated. All spin-coated films [Figure 5.8a–d, Series (1)] show virtually identical spectra with well-resolved features and maxima at ≈ 470 and ≈ 508 nm. The spectral shape is indicative of emission from well dispersed – as opposed to aggregated – PPE molecules, [12a] suggesting that rapid solvent evaporation during spin-coating produces kinetically-trapped, molecularly-mixed PS/EHO-OPPE blends. Presumably due to the less polar nature of PS as the solid solvent, the emission spectra are slightly blue-shifted compared to those recorded in DCE and CF solution (Figure 5.7). The emission spectra of the solution-cast films [Figure 5.8a–d, Series (2)] paint a slightly different picture. Here, two major bands centered at ≈ 465–473 and 529 nm are observed. While the former coincides with the high-energy band observed in the spin-coated films and appears to be associated with emission from well-dispersed PPE molecules, the latter suggests emission from a neat (but disordered) PPE phase.[12a,13c] This finding reflects that slow solvent evaporation results in phase-separated PS/EHO-OPPE blends, indicative of thermodynamic immiscibility of the two polymers.

A comparison of the PL emission spectra of pristine e-spun fibers [Figure 5.8a–d, Series (3)] with those of the spin-coated and the solution-cast films shows that the fiber emission is virtually exclusively due to emission from a phase-separated PPE phase. Assuming that annealing above the T_gs of the polymers (95 °C for PS; 90 °C for EHO-OPPE[12b]) could change the morphology (and therewith the optical properties) of the blends, the e-spun nanofibers were annealed for up to 1 h at 110 °C. The effect of thermal annealing on the emission spectra is reflected by the spectra shown in Figure 5.8a–d, Series 4–6. Interestingly, annealing leads to the appearance of an emission band around ≈ 465–470 nm, the intensity of which increases with the annealing time. This finding is consistent with an increased miscibility of the two polymers at higher temperature, causing at least a minor portion of the conjugated polymer molecules to disperse in the PS host upon

annealing. Obviously, that morphology is maintained when the samples are cooled to room temperature.

Table 5.3 Summary of the positions of peaks and shoulders of the PL emission spectra of 8.5% (w/v) solutions of PS/EHO-OPPE (PS:EHO-OPPE = 7.5:1) in DCE and CF without and with the addition of 8 vol.-% PF, the corresponding spin-coated and solution-cast films, and the as-annealed (i.e., at 110 °C) PS/EHO-OPPE fibers

Samples	System	Annealing Time (min)	Peaks (nm)		Shoulders (nm)	
			High Intensity	Low Intensity	High Energy	Low Energy
Solutions	DCE	-	487	509	-	-
	DCE + PF	-	487	508	-	-
	CF	-	485	506	-	-
	CF + PF	-	485	508	-	-
Spin-coated films	DCE	-	470	-	490	-
	DCE + PF	-	470	-	490	-
	CF	-	470	-	489	-
	CF + PF	-	470	-	489	-
Solution-cast films	DCE	-	463	529	-	-
	DCE + PF	-	462	529	-	-
	CF	-	463	528	-	-
	CF + PF	-	462	528	-	-

Table 5.3 (Cont.) Summary of the positions of peaks and shoulders of the PL emission spectra of 8.5% (w/v) solutions of PS/EHO-OPPE (PS:EHO-OPPE = 7.5:1) in DCE and CF without and with the addition of 8 vol.-% PF, the corresponding spin-coated and solution-cast films, and the as-annealed (i.e., at 110 °C) PS/EHO-OPPE fibers

Samples	System	Annealing Time (min)	Peaks (nm)		Shoulders (nm)	
			High Intensity	Low Intensity	High Energy	Low Energy
E-spun fibers	DCE	0	503	-	468	594
		5	503	-	473	595
		30	505	-	473	594
		60	505	-	473	595
	DCE + PF	0	516	-	465	594
		5	515	-	469	595
		30	513	-	465	594
		60	507	-	465	596
	CF	0	516	-	464	595
		5	514	-	464	594
		30	509	-	469	594
		60	507	-	470	593
	CF + PF	0	519	-	466	595
		5	517	-	470	594
		30	511	-	469	595
		60	510	-	470	594

Table 5.4 Summary of the positions of peaks and shoulders of the PL emission spectra of the electrospun fibers from 8.5% (w/v) solutions of PS/EHO-OPPE (PS:EHO-OPPE = 7.5:1) in DCE and CF with 8 vol.-% PF at various applied electrical potentials (HV)

Solution	HV (kV)	Peak (nm)	Shoulders (nm)	
			High Energy	Low Energy
PS/EHO-OPPE /DCE + PF	7.5	517	460	595
	10.0	515	461	599
	12.5	510	457	591
	15.0	516	458	594
	17.5	515	459	595
	20.0	516	460	596
PS/EHO-OPPE /CF+ PF	7.5	508	460	590
	10.0	511	460	593
	12.5	514	457	591
	15.0	519	459	595
	17.5	515	458	594
	20.0	511	459	596

5.4.3 Morphology of the Annealed E-spun Fibers

Figure 5.9 shows representative SEM images of the e-spun PS/EHO-OPPE fibers that had been annealed for 1 h. Minor morphological changes are evident. Many fused sections can be observed and some parts of the annealed fibers flattened into ribbons. Moreover, the size of the annealed fibers is slightly larger when compared with that of the pristine fibers (see Table 5.5), a result that is consistent with the expansion of the fused sections.

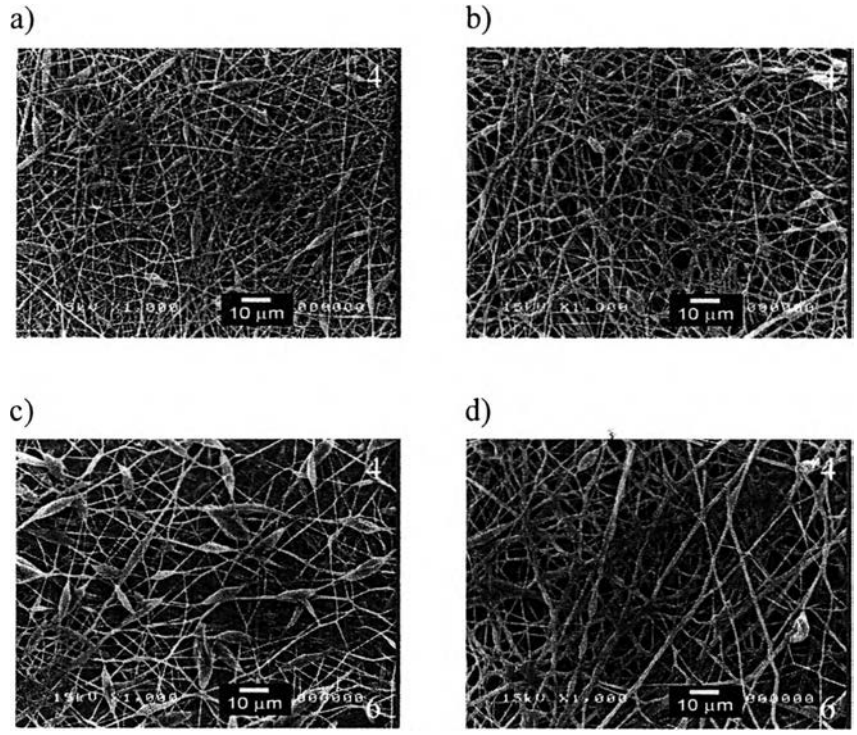

Figure 5.9 SEM images of the as-annealed fibers (1 h at 110 °C) electrospun from 8.5% (w/v) solutions of PS/EHO-OPPE (PS:EHO-OPPE = 7.5:1) in a) DCE, b) DCE with the addition of 8 vol.-% PF, c) CF and d) CF with the addition of 8 vol.-% PF (×1,000, scale bar = 10 µm).

Table 5.5 Average fiber diameter, bead size and bead density of the electrospun fibers from 8.5% (w/v) solutions of PS/EHO-OPPE (PS:EHO-OPPE = 7.5:1) in a) DCE, b) DCE with 8 vol.-% PF, c) CF, and d) CF with 8 vol.-% PF. The fibers were electrospun at an applied electrical potential of 15 kV and then annealed for 1 h at 110 °C

Annealed Fibers	Fiber Diameters (μm)	Bead Size (μm)	Bead Density (beads·cm^{-2})
PS/EHO-OPPE /DCE	0.82 ± 0.25	2.79 ± 1.22	3.26×10^5
PS/EHO-OPPE /DCE + PF	0.76 ± 0.31	3.53 ± 1.52	1.76×10^5
PS/EHO-OPPE /CF	0.68 ± 0.28	6.45 ± 1.11	3.74×10^5
PS/EHO-OPPE /CF + PF	1.15 ± 0.45	3.71 ± 1.34	1.21×10^5

5.5 Conclusions

In this work, ultra-fine PS/EHO-OPPE fibers with average diameters ranging from 430 to 1,200 nm were successfully prepared by electrospinning the solutions of 8.5 wt.-% PS/EHO-OPPE (PS/EHO-OPPE = 7.5:1 w/w) in 1,2-dichloroethane (DCE) and chloroform (CF) with and without the addition of pyridinium formate (PF). While the increase in the electrical potential resulted in the observed increase in the diameters of the e-spun fibers, the addition of PF significantly improved the electro-spinnability of the resulting PS/EHO-OPPE solutions, as shown by the decrease in the bead density of the obtained fibers. FT-IR spectroscopy showed that the chemical structure of PS and EHO-OPPE did not change and still existed in the e-spun fibers. The optical properties (e.g., absorption and emission) of the as-prepared solution, the e-spun fibers, the annealed fibers, and

both the spin-coated and the solution-cast reference films were studied by UV-vis and PL spectroscopy. A red-shift was observed in emission spectra of the e-spun fibers and the solution-cast films when compared with those of the corresponding solutions. This shift could be attributed to the phase separation of the EHO-OPPE molecules, which resulted in a higher degree of molecular interaction. The shift in the e-spun fibers was less pronounced when they were annealed. Presumably, this was due to increased PPE mobility to disperse much more evenly in the PS matrix, resulting in even lesser aggregation or the destruction of the precedent aggregation.

5.6 Acknowledgments

PS acknowledges partial support received from the Thailand Research Fund (TRF) (through a research career development grant: RMU4980045), the National Center of Excellence for Petroleum, Petrochemicals, and Advanced Materials (NCE-PPAM), and the Petroleum and Petrochemical College (PPC), Chulalongkorn University. SC acknowledges a doctoral scholarship received from the Royal Golden Jubilee PhD Program, through the Thailand Research Fund (TRF). CW acknowledges support received from the National Science Foundation (under grant no. DMR-0215342). We thank Michael Schroeter for the synthesis of EHO-OPPE.

5.7 References

[1] E. Shirakawa, E. J. Louis, A. G. MacDiarmid, C. K. Chiang, A. J. Heeger, J Chem Soc Chem Comm 1977, 579.

[2] [2a] A. J. Heeger, Rev. Mod. Phys. 2001, 73, 681; [2b] A. G. MacDiarmid, Rev Mod Phys 2001, 73, 701; [2c] H. Shirakawa, Rev Mod Phys 2001, 73, 713.

[3] [3a]"Handbook of Organic Conductive Molecules and Polymers", H. S. Nalva, Ed., Wiley, New York 1997; [3b] T. A. Skoetheim, R. L. Elsenbaumer, J. R. Reynolds, Eds., "Handbook of Conducting Polymers", Dekker, New York 1998.

[4] [4a] J. H. Burroughes, D. D. C. Bradley, A. R. Brown, R. N. Marks, K. Mackay, R. H. Friend, P. L. Burns, A. B. Holmes, Nature 1990, 347, 539; [4b] A. Kraft, A. C. Grimsdale, A. B. Holmes, Angew Chem Int Ed 1998, 37, 402; [4c] U. Mitschke, P. Bäuerle, J Mater Chem 2000, 10, 1471; [4d] A. Greiner, C. Weder, in: "Encyclopedia of Polymer Science and Technology", J. I. Kroschwitz, Ed., Wiley-Interscience, New York 2003, p. 87.

[5] G. Horowitz, Adv Mater 1998, 10, 365.

[6] C. J. Brabec, N. S. Sariciftci, J. C. Hummelen, Adv Funct Mater 2001, 11, 15.

[7] D. T. McQuade, A. E. Pullen, T. M. Swager, Chem Rev 2000, 100, 2537.

[8] F. R. Denton, III, P. M. Lahti, "Photonic Polymer Systems - Fundamentals, Methods, and Applications", D. L. Wise, G. E. Wnek, D. J. Trantolo, T. M. Cooper, J. D. Gresser, Eds., CRC Press, New York 1998.

[9] U. Scherf, E. J. W. List, Adv Mater 2002, 14, 477.

[10] "Poly(Arylene Ethynylene)s – From Synthesis to Applications", C. Weder, Ed., Adv Polym Sci Series, Vol. 177, 2005.

[11] [11a] C. Weder, M. S. Wrighton, R. Spreiter, C. Bosshard, P. Gunter, J Phys Chem 1996, 100, 18931; [11b] G. S. He, C. Weder, P. Smith, P. N. Prasad, IEEE J Quantum Electron 1998, 34, 2279.

[12] [12a] C. Weder, M. S. Wrighton, Macromolecules 1996, 29, 5157; [12b] D. Steiger, P. Smith, C. Weder, Macromol Rapid Commun 1997, 18, 643; [12c] S. Dellsperger, F. Dotz, P. Smith, C. Weder, Macromol Chem Phys 2000, 201, 192; [12d] D. Knapton, P. K. Iyer, S. J. Rowan, C. Weder, Macromolecules 2006, 39, 4069.

[13] [13a] A. Montali, P. Smith, C. Weder, Synth Met 1998, 97, 123; [13b] C. Schmitz, P. Pösch, M. Thelakkat, H. W. Schmidt, A. Montali, K. Feldman, P. Smith, C. Weder, Adv Func Mater 2001, 11, 41; [13c] M. Burnworth, J. D. Mendez, M. Schroeter, S. J. Rowan, C. Weder, Macromolecules 2008, 41, 2157.

[14] [14a] A. Kokil, I. Shiyanovskaya, K. D. Singer, C. Weder, J Am Chem Soc 2002, 124, 9978; [14b] A. Kokil, I. Shiyanovskaya, K. D. Singer, C. Weder, Synth Met 2003, 138, 513.

[15] [15a] A. Kokil, P. Yao, C. Weder, Macromolecules 2005, 38, 3800; [15b] P. K. Iyer, J. B. B. Beck, C. Weder, S. J. Rowan, Chem Comm 2005, 319.

[16] G. Voskerician, C. Weder, Adv Polym Sci 2005, 177, 209.

[17] [17a] C. Weder, C. Sarwa, C. Bastiaansen, P. Smith, Adv Mater 1997, 9, 1035; [17b] A. Montali, G. Bastiaansen, P. Smith, C. Weder, Nature 1998, 392, 261; [17c] A. R. A. Palmans, M. Eglin, A. Montali, C. Weder, P. Smith, Chem Mater 2000, 12, 472.

[18] C. Weder, C. Sarwa, A. Montali, C. Bastiaansen, P. Smith, Science 1998, 279, 835.

[19] Y. Xu, P. R. Berger, J. N. Wilson, U. H. F. Bunz, Appl Phys Lett 2004, 85, 4219.

[20] H. Hoppe, N. S. Sariciftci, D. A. M. Egbe, D. Mühlbacher, M. Koppe, Mol. Cryst. Liq. Cryst. 2005, 426, 255.

[21] D. Knapton, M. Burnworth, S. J. Rowan, C. Weder, Angew Chem Int Ed 2006, 45, 5825.

[22] [22a] E. Hittinger, A. Kokil, C. Weder, Angew Chem Int Ed 2004, 43, 1808; [22b] E. Hittinger, A. Kokil, C. Weder, Macromol Rapid Commun 2004, 25, 710.

[23] [23a] J. X. Jiang, F. Su, A. Trewin, C. D. Wood, N. L. Campbell, H. Niu, C. Dickinson, A. Y. Ganin, M. J. Rosseinsky, Y. Z. Khimyak, A. I. Cooper, Angew Chem Int Ed 2007, 46, 8574; [23b] C. Weder, Angew Chem Int Ed 2008, 47, 448.

[24] Y. Wang, J. S. Park, J. P. Leech, S. Miao, U. H. F. Bunz, Macromolecules 2007, 40, 1843.

[25] P. Wutticharoenmongkol, P. Supaphol, T. Srikhirin, T. Kerdcharoen, T. Osotchan, J Polym Sci, Part B: Polym Phys 2005, 43, 1881.

[26] H. Wang, X. Lu, Y. Zhao, C. Wang, Mater Lett 2006, 60, 2480.

[27] N. Dharmaraj, C. H. Kim, K. W. Kim, H. Y. Kim, E. K. Suh, Spectrochim Acta A 2006, 64, 136.

[28] R. Luoh, H. T. Hahn, Compos Sci Technol 2006, 66, 2436.

[29] S. Tungprapa, I. Jangchud, P. Ngamdee, M. Rutnakornpituk, P. Supaphol, Mater Lett 2006, 60, 2920.

[30] X. Li, X. Hao, D. Xu, G. Zhang, S. Zhong, H. Na, D. Wang, J Membrane Sci 2006, 281, 1.

[31] Y. C. Ahn, S. K. Park, G. T. Kim, Y. J. Hwang, C. J. Lee, H. S. Shin, J. K. Lee, Curr Appl Phys 2006, 6, 1030.

[32] J. S. Jeong, J. S. Moon, S. Y. Jeon, J. H. Park, P. S. Alegaonkar, J. B. Yoo, Thin Solid Films 2007, 515, 5136.

[33] D. Kawaguchi, K. Tanaka, A. Takahara, T. Kajiyama, Macromolecules 2001, 34, 6164.

[34] T. Jarusuwannapoom, W. Hongrojjanawiwat, S. Jitjaicham, L. Wannatong, M. Nithitanakul, C. Pattamaprom, P. Koombhongse, R. Rangkupan, P. Supaphol, Eur Polym J 2005, 41, 409.

[35] C. Mit-Uppatham, M. Nithitanakul, P. Supaphol, Macromol Chem Phys 2004, 205, 2327.

[36] S. Chuangchote, T. Srikhirin, P. Supaphol, Macromol Rapid Commun 2007, 28, 651.

[37] H. Fong, I. Chun, D. H. Reneker, Polymer 1999, 40, 4585.

[38] Z. M. Huang, Y. Z. Zhang, M. Kotaki, S. Ramakrishna, Compos Sci Technol 2003, 63, 2223.